Chapter 5
Analysis of Test Results

This chapter is intended to discuss and analyze the experimental results of the test columns. An evaluation is presented for the key column variables that affect the seismic behavior of HSC columns designed according to the seismic requirement of the ACI 318. The following discussion includes the effect of the steel fibers content, concrete compressive strength, axial load level, ties yield strength and confinement index, on the specimen's behavior including the column capacity and the ductility characteristics. The observed lateral load-displacement responses of the column specimens are grouped for each column variable.

5.1 Steel Fibers Content

Three groups were tested to study the effect of the amount of steel fibers on the behavior of columns with nominal concrete strength of 50, 75 and 100 N/mm^2 Fig. 5-1. The concrete mix of each group contained 0.00, 0.75, and 1.50% volumetric ratio of the steel fibers (volume of steel fibers in one cubic meter of concrete). In general, provision of the steel fibers is shown in Fig. 5-2 to enhance the cracking and ultimate capacities, and the ductility of the test columns. The enhancement declines with increasing the concrete strength of the specimen, Fig. 5-1.

For specimens with concrete compressive strength of 50 N/mm^2, the test results show significant improvement in the cracking and ultimate load-carrying capacities of FRHSC columns. Compared to Specimen C1, the increase in the cracking load was 46% and 58%, and in the ultimate load was 26% and 29% for Specimens C2 and C3, respectively, Fig. 5-2. Fig. 5-1a shows the load displacement envelope of Specimens C1, C2 and C3. As shown, the specimens provided with steel fibers exhibited more ductile behavior compared to that of

Specimen C1. Specimens C2 and C3 had an initial stiffness of 32% and 40%, respectively more than that of Specimen C1, Fig 5-3. The energy index of Specimens C2 and C3 were increased by 13% and 36%, respectively, refer to Fig. 5-4. The plastic hinge extent decreased as the steel fibers ratio increased. The length of the plastic hinge developed in Specimens C2 and C3 was 81% and 50%, respectively of that of Specimen C1, Fig. 5-5.

As far as specimens with concrete strength of 75 N/mm^2 are concerned, the increase in the cracking and ultimate load was 13% and 17%, respectively for Specimen C5 (V_f = 0.75%) whereas the corresponding enhancement for Specimen C6 (V_f = 1.5%) was 39% and 20%, respectively, Fig. 5-2. Fig. 5-1b shows the load displacement response of Specimens C4, C5 and C6. The energy dissipation capacity of Specimens C5 and C6 was 72% and 76%, respectively, higher than that of Specimens C4; refer to Fig. 5-4. The initial stiffness of Specimens C5 and C6 increased by 10% and 16%, respectively, and the displacement ductility improved by 14% and 22%, respectively, Fig. 5-6. The extent of the plastic hinge of Specimens C5 and C6 was 86% and 50% of that of Specimen C4.

Test results of specimens with concrete compressive strength of 100 MPa reveal that the cracking load increased by 17% and 27%, for specimens with 0.75% and 1.5% steel fibers ratio, whereas the enhancement in the ultimate load was 15% and 19%, respectively. The energy dissipation capacity of Specimens C8 and C9 was about five times that of Specimens C7. Specimens C8 and C9 had an initial stiffness of 112% and 115%, respectively, of Specimen C7. Fig. 5-1c shows the load displacement envelope of Specimens C7, C8 and C9. As shown, provision of steel fibers increases the displacement ductility by about 76% and the drift ratio by 47%. The rate of strength decay and stiffness degradation considerably decreased for these specimens. The length of the plastic hinge developed in Specimens C8 and C9 represented 73% and 55% of that of Specimen C7, respectively.

The improvement in the cracking and ultimate load-carrying capacity due to the steel fibers are superior in increasing the tensile and bond strength as well as the confinement of the concrete core. The fibers across cracks carry tensile forces and hence affect the concrete core by a passive stress that improve the core confinement and add to the energy dissipation capacity. Abu Dayya (2002) reported that the steel fibers significantly increase the initial secant stiffness value of the beam-column joints specimens and provide a stable reduction in secant stiffness. Shannag *et al*. (2005) reported a twenty three times increase in the dissipated energy of the beam-column joints specimens with increasing the fiber ratio from 0.0% to 4.0%. Kimura *et al*. (2007) in their experimental study on HSC column of 200 MPa concrete strength observed that the flexural strength of specimens with 1.0% steel fibers ratio enhanced by 47% as the addition of fibers prevents the separation between concrete core and cover. Under cyclic loading, Lee, H. (2007), tested columns specimens with 24 MPa concrete compressive strength and 2.0% maximum steel fibers. The results of tests indicated that the steel fibers were more effective in improving the strength and ductility capacity than the stiffness and energy capacity of the column. Similar observation was reported by Takatsu *et al*. (2006). Paultre *et al*. (2008) tested six NSC circular columns of 30 MPa under lateral load and constant axial load, the axial load was 0.25 of axial load capacity. The result of test demonstrated that with a volumetric fiber ratio of 1.0%, improvements in ductility and energy dissipation capacities are obtained compared to similar specimens made of NSC. However, this improvement is less visible when higher amounts of confinement steel are used. Reduction of the amounts of confinement steel seems to be possible when using FRNSC.

5.2 Concrete Compressive Strength

Test results on ten specimens; C1 to C9 and C13, were analyzed to demonstrate the effect of concrete compressive strength on the column behavior. The specimens were tested under an axial load of *0.25N/fc'Ag*. All the specimens were

designed based on the minimum requirements of the seismic provisions of ACI 318 as set on the transverse reinforcement, except Specimen C13 which had 80% additional capacity of the transverse steel. The observed lateral load-displacement responses of the specimens are illustrated in Figs. 5-7. The results are grouped for the specimens with identical column parameters but with variable concrete strength.

Fig. 5-7a shows the load-displacement response of specimens without steel fibers; Specimens C1, C4 and C7. The load carrying capacity of the specimens is shown to be significantly increased with increasing the concrete strength. Increasing the concrete compressive strength from 51.3 MPa to 73.0 MPa and 94.7 MPa resulted in 50% and 76% increase in the cracking load, respectively, and in 20% and 44% enhancement in the ultimate load, respectively, Fig 5-2. Obviously, the cracking capacity depends mainly on the concrete strength whereas the ultimate flexural capacity is significantly affected by the reinforcement content. Specimen C1 with 51.3 MPa concrete strength displayed superior energy dissipation characteristics and behaved in a more ductile manner compared to Specimens C4 and C7. The energy index of Specimen C1 was 1.92 and 5.17 of that of Specimen C4 and C7, respectively, Fig. 5-4. The extent of the plastic hinge developed in Specimen C1 was 160 mm representing about 1.15 and 1.45 times that of Specimen C4 and C7, respectively, Fig. 5-5. The displacement ductility and drift ratios recorded confirm the brittle behavior of the specimens with high concrete strength. The results indicate that the displacement ductility was 6.2, 3.6 and 2.5 for the specimens with concrete strength of 51.3, 73.0 and 94.7 MPa, respectively, while the corresponding drift ratio was 3.9, 2.5 and 1.5, respectively, Fig. 5-6. It can be concluded that in HSC columns subjected to cyclic lateral load as the concrete strength increases, the displacement ductility and drift ratio decreases. Furthermore, the normalized dissipated energy index decreases as the concrete strength increases. Similar observations were recorded by Bayrak and Sheikh (1998). Overall, columns that had approximately 50 MPa concrete and axial loads level of 25 percent of column axial load capacity, and that were designed based on

seismic provisions of ACI 318, exhibited adequate ductility. Columns with concrete compressive strength about 75 MPa and with axial load beginning from 25 percent of column axial load capacity require higher amounts of transverse reinforcement than required by seismic provisions of ACI 318 to attain the ductility level intended by the code.

To a lesser extent, a comparable effect of the concrete compressive strength on the column specimens provided with 0.75% fiber content; Specimens C2, C5 and C8, was recorded. Compared to Specimen C2, the increase in the cracking load of Specimens C5 and C8 was 17% and 41%, respectively, whereas the increase in the ultimate capacity was 12% and 32%, respectively. Again, Specimen C2 with 53.8 MPa concrete strength displayed better energy dissipation compared to Specimens C5 and C8. The displacement ductility ratios recorded confirm the ductile behavior of all the specimens due to presence of the steel fibers, Fig. 5-7b. The length of the plastic hinge developed in Specimen C2 was 8% and 62% more than that of Specimens C5 and C8, respectively. The energy index of Specimen C2 was 27% and 16% higher than that of Specimens C5 and C8, respectively. The test results reveal a decline in the drift ratio from 3.5 to 2.2 with increasing the concrete strength increase from 53.8 to 98.6 MPa. The displacement ductility ratios of all the specimens were nearly equal, Fig.5-6.

As far as the column specimens provided with 1.5% fibers content; Specimens C3, C6 and C9, are concerned, increasing the concrete strength from 54.5 MPa to 99.8 MPa resulted in an increase in the cracking and ultimate load by 42% and 33%, respectively. Specimen C3 with 54.5 MPa concrete strength displayed better energy dissipation characteristics and behaved in a more ductile manner compared to Specimens C6 and C9, see Fig. 5-7c. The energy index of Specimen C3 was 1.48 and 1.33 of that for Specimens C6 and C9, respectively. The plastic hinge developed in Specimen C3 extended over a length being 14% and 33% more than that of Specimens C6 and C9, respectively, Fig.5-5. The drift ratio dropped from 3.8 to 2.1 with increasing the concrete strength from 54.5 to 99.8 MPa. The

displacement ductility ratios of all the specimens were equal.

A close examination of the load-displacement response for Specimens C9 and C13 shown in Fig. 5-7c reveals that the concrete compressive strength has a significant effect on the post-peak response of the test columns. Unlike the previous groups, the change in the column behavior is attributed only to the concrete strength. The results indicate that Specimen C13 with transverse reinforcement of 80% more than the minimum required by ACI 318, developed significantly higher deformability compared to Column C9 although the initial stiffnesses were comparable. The cracking and ultimate capacities of these specimens were practically unchanged. The energy index of Specimen C13 was about 2.5 times that of Specimen C9. The extent of the plastic hinge in Specimen C9 was about 1.2 times that of Specimen C13. With increasing the concrete compressive strength from 77.3 MPa to 99.8 MPa the displacement ductility decreased from 7.0 to 4.3 and the drift ratio from 3.5 to 2.1, see Fig. 5-6. Daniel and Loukili (2002), reported that the increase in the loading capacity of FRHSC columns lead to a steeper slope of the post peak behavior.

Sheikh and Khoury (1991) and Sheikh *et al*. (1994) observed lower ductility in HSC columns as compared to NSC columns concluding that the required amount of tie steel for a given performance of a column under a certain axial load level is proportional to the concrete strength. For bending accompanied by axial compression, the increase in the amount of tie steel for HSC columns is not needed to compensate for the loss of strength due to cover spalling but to maintain the integrity of the column core to provide ductile behavior.

5.3 Axial Load Level

Axial load had a significant influence on the performance of HSC columns under seismic loading with particular reference to the ductility characteristics. The presence of a moderate value of axial force increases the cracking moment,

flexural stiffness and moment capacity of a reinforced concrete section. Such effects may be partially offset by the geometrical nonlinear conduct of the member, which magnifies the bending moments sustained by the member. In order to study the influence of the axial load level on the behavior of FRHSC columns, test results on Specimens C6, C9, C10, C12 and C14 were analyzed. These specimens had identical column parameters with concrete compressive strength of 75MPa and 100 MPa, and subjected to axial load of 0.10, 0.25 or 0.45 of the axial load capacity. Fig 5-8 indicates the lateral load displacement responses of the specimens as grouped according to the concrete strength.

For the specimens with nominal concrete strength of 75 MPa, the load carrying capacity is shown in Fig. 5-8a to increase significantly with increasing the applied axial load from 0.10 to 0.45 of the axial load capacity. The increase in the cracking and ultimate load was 51% and 37%, respectively, Fig. 5-2. In addition, increasing the axial load level from 10 to 45 percent reduced the ultimate displacement from 16 mm to 10.5 mm. Similar observations were recorded for HSC columns by Azizinamini *et al.* (1994) and Xiao and Yun (2002). The results indicated that for normal strength concrete columns increasing the axial load level from 20 to 40 percent reduced the maximum displacement by 30 percent and for HSC columns increasing the axial load level from 20 to 30 percent reduced the maximum displacement by 17 percent.

The energy index for the specimen subjected to 10% axial load level; Specimen C12 was about 3.9 and 21.6 times that of specimens tested under 25% and 45% axial load level; Specimens C6 and C14, respectively, see Fig. 5-4. On the other hand, the strength decay rate; SDR increased with increasing the applied axial load level. SDR is shown in Table 4-3 to be 3.1, 3.5 and 10.1 KN/mm for the specimens subjected to 10, 25 and 45 percent load level; respectively. Bayrak and Sheikh (1996) observed that high axial load levels resulted in an increase in the rate of stiffness degradation with every load cycle, and adversely affected the cyclic performance of HSC columns. The displacement ductility and drift ratios

recorded confirm the brittle behavior of the specimen tested under high axial load level. The displacement ductility was 7.9, 4.4 and 3.1 for an axial load level of 10, 25 and 45 percent, respectively, whereas the corresponding drift ratio was 3.9, 3.0 and 2.1, respectively. In conclusion, the column subjected to low levels of axial load was able to sustain reasonable inelastic cyclic displacement. As the axial load increases, however, the behavior shows an insufficient level of ductility and energy dissipation capacity for seismic applications.

Sheikh *et al*. (1994) accepted that ACI requirements on confinement reinforcement are not conservative in case of highly axially loaded columns, and rather conservative and uneconomical in a great number of situations of practical interest in which columns support low axial compression. According to Saatcioglu and Baingo (1999), the deformability of HSC columns decreases with increasing the axial compression, and the lateral drift capacity increases when the level of axial load decreases. Bayrak and Sheikh (1998) reported that an increase in the axial load reduces the column deformability and ductility, and accelerates strength and stiffness degradation. To compensate for such adverse effects, a larger amount of lateral reinforcement was recommended. Therefore, they suggested incorporation of the axial load level as a design parameter in the design of the confinement reinforcement. The need to include the axial load level in the code requirements for confinement reinforcement was also pointed out by Legeron and Paultre (2000). It is believed, however, that the presence of steel fibers may ease the required reinforcement in HSC columns subjected to high levels of axial load, refer to test results of Specimen C14.

Comparable conduct was observed for specimens with nominal concrete strength of 100 MPa; Specimens C9 and C10 as shown in Fig. 5-8b. The load carrying capacity is shown to increase with increasing the applied axial load from 0.10 to 0.25 of the axial load capacity. The increase in the cracking and ultimate load was 39% and 19%, respectively, whereas the reduction in the ultimate displacement was about 60%. The energy index for the specimen subjected to 10% axial load

level (Specimen C10) was about 1.24 times that of the specimen tested under 25% axial load level (Specimen C9). The latter had a strength decay rate of 30% higher. The test results reveal that the displacement ductility was 4.6 and 4.3 at an axial load level of 10% and 25%, respectively and the corresponding drift ratio was 3.4 and 2.1, respectively. A close examination of these results reveals that when the level of axial load is above 25 percent of the column axial load capacity and the concrete strength is approximately 100 MPa, larger amounts of transverse reinforcement, than specified in the seismic provisions of ACI 318, are required. This agrees with the recommendation of ACI 441 on columns with concrete strength approximately 100 MPa and with axial load level above 30%. Paultre *et al.* (2009) tested six HSC circular columns of 100 MPa under an axial load ranging from 0.15 to 0.40 of the axial load capacity. The result demonstrated that HSC columns designed according to CSA (2004) can achieve adequate ductility if the transverse reinforcement was designed to account for the axial load level and the yield strength of transverse steel.

5.4 Yield Strength of Transverse Reinforcement

Conflicting views on the effectiveness of using high strength steel as confinement reinforcement have been reported in literature on HSC columns [Wang *et al*. (1995) and Hwang and Yun (2004)]. In this section, test result on Specimens C6 and C13 were analyzed to investigate the effect of the yield strength of transverse reinforcement on the column behavior. The yield strength of the transverse reinforcement for Specimens C6 and C13 was 274 N/mm^2 and 516 N/mm^2, respectively. The lateral load-displacement relationship is shown in Fig. 5-9.

The results indicate that the specimen provided with ties of high grade steel exhibited significantly higher deformability in the post peak response. The increase in the initial stiffness, however, was 36%, refer to Fig. 5-3. The increase in the cracking and ultimate load due to increasing the tie yield strength from 274 MPa to 516 MPa, was 9% and 19%, respectively. The enhancement in the energy

index was about 180%. The extent of the plastic hinge developed at failure in Specimen C6 was about 1.4 times that of Specimen C13. Referring to Fig. 5-6 increasing the yield strength from 274 N/mm^2 to 516 N/mm^2 raised the displacement ductility from 4.4 to 7.0 and the drift ratio from 3.0 to 3.5.

Saatcioglu and Baingo (1999) accepted that the increased confinement required for HSC columns subjected to axial load level ranging from 22% to 43% can be provided by increasing the volumetric ratio and/or yield strength of transverse steel. Xiao and Yun (2002) reported for HSC columns tested under axial load level ranged from 20% to 34% that, the use of high strength transverse reinforcement was found to be effective in providing additional confinement and ductility. However, earlier investigation showed that using ties of high yield strength may not be efficient for every column configuration [Park *et al.* (1998)]. At low level of axial load, however, one reason for using high grade transverse reinforcement in HSC columns is to allow larger spacing of ties [Azizinamini *et al*. (1994)].

5.5 Confinement Index

This section presents a discussion on the significance of the confinement index $\rho_s f_{yh}/f_c'$ on the behavior of HSC columns. The factor $\rho_s f_{yh}/f_c'$ has been recommended by ACI 441 to evaluate the confinement efficiency. Test results on Specimens C6, C11 and C13 were investigated to evaluate the effectiveness of the confinement index. The confinement index values were 0.122, 0.392 and 0.230. Fig. 5-10 shows the load-displacement response of these specimens. The increase in the cracking load, the confinement index increased from 0.122 to 0.392, was about 11% and the corresponding enhancement in the ultimate load was 24%, Fig. 5-2. Specimens C11 and C13 had an initial stiffness of 56% and 36%, respectively more than that of Specimen C6. The energy index and the displacement ductility for the Specimen C6 were about 0.36 and 0.63 times that of the other specimens. With increasing the confinement index from 0.122 to 0.392 the drift ratio

increases from 3.0 to 4.0, Fig. 5-6.

Paultre *et al.* (2001) pointed out that the ductility of HSC columns being dependent on concrete strength and the amount of lateral steel, can be decreased provided that the yield strength of the lateral steel is increased. Hence, a trade-off exists between yield strength and amount of lateral steel. They believed, however, that ties of high yield strength may not be effective in every case. When columns are poorly confined, high yield strength is not totally effective and the yield strength should not be taken into account. Saatcioglu and Baingo (1999) suggested that the ratio $\rho_s f_{yh}/f_c'$ can be used as a design parameter for the confinement of HSC columns. Hwang and Yun (2004), on the other hand, reported that the influence of the volumetric ratio of transverse steel is a more leading parameter in controlling the column response.

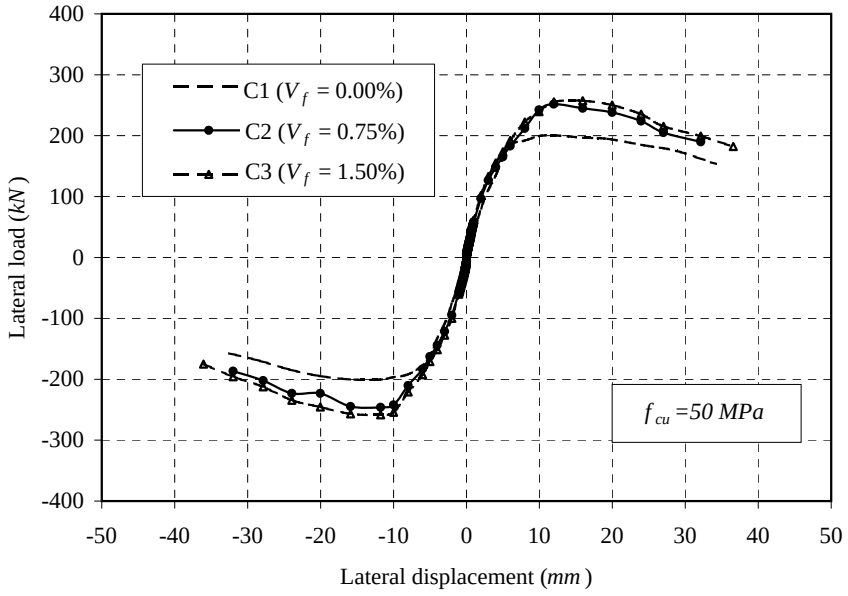

a)

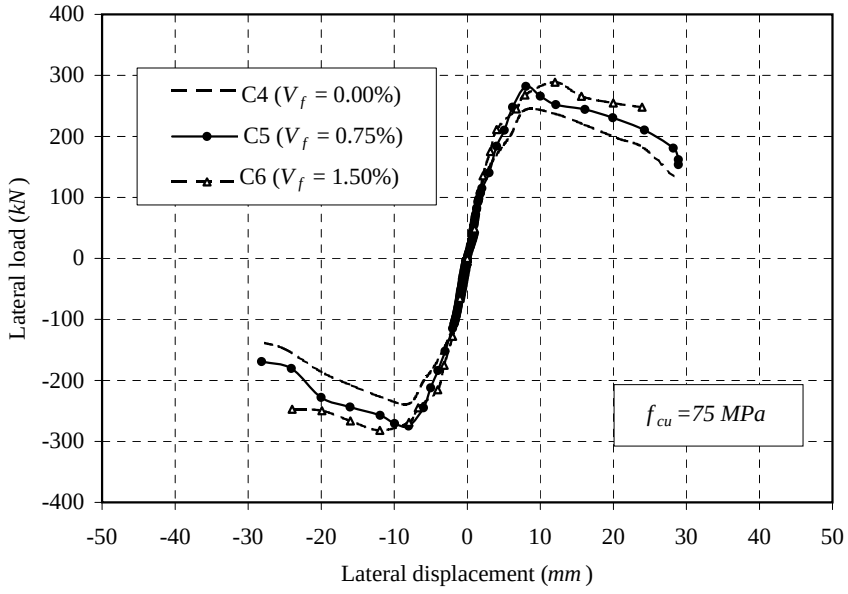

b)

Fig. 5-1 Effect of fiber content on load-displacement response of specimens with nominal concrete strength: a) 50 MPa; b) 75 MPa; c) 100 MPa

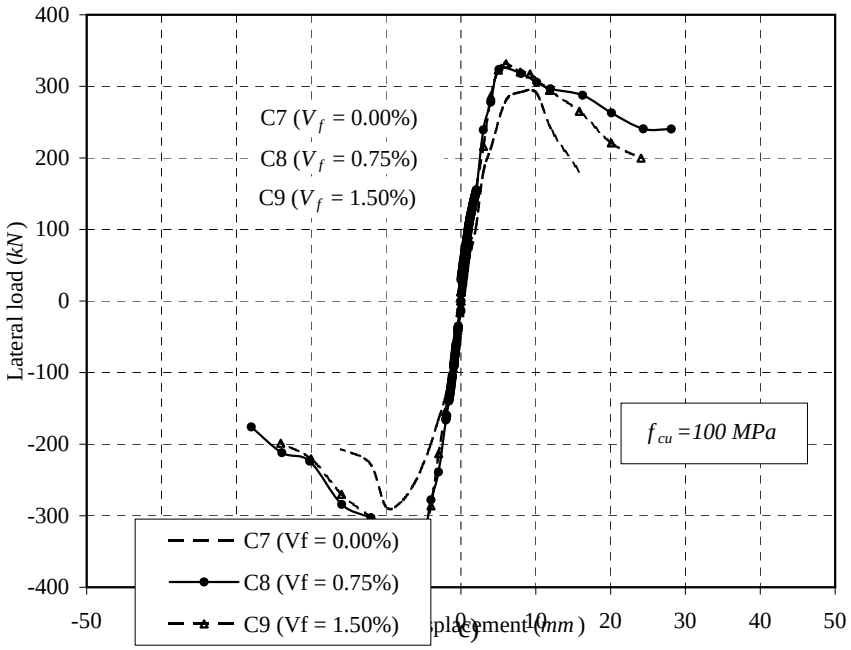

Fig. 5-1 Effect of fiber content on load-displacement response of specimens with nominal concrete strength: a) 50 MPa; b) 75 MPa; c) 100 MPa (cont.)

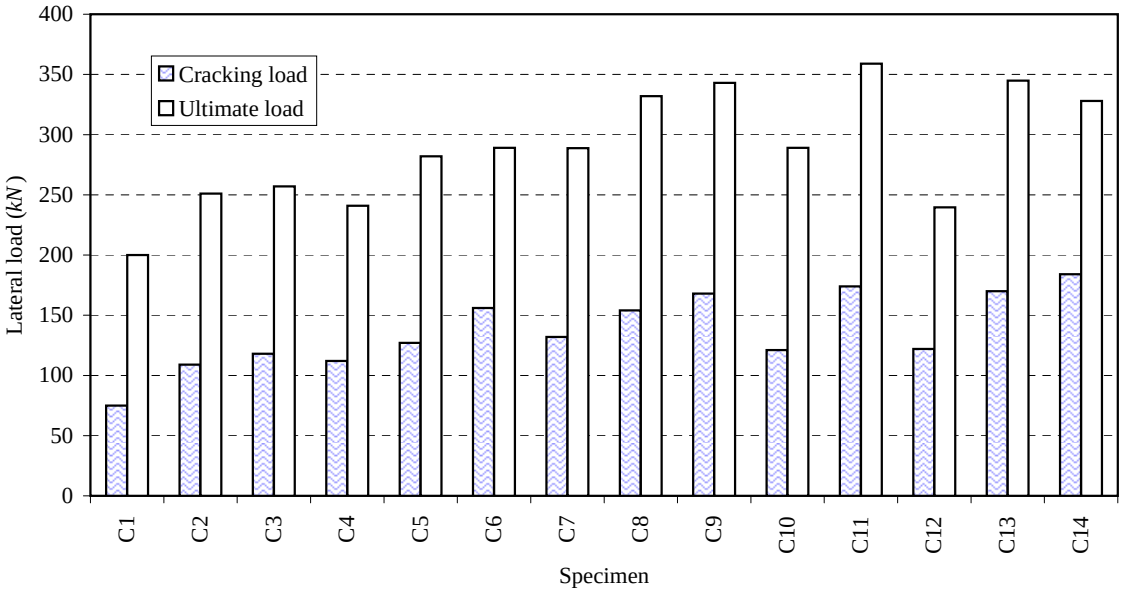

Fig. 5-2 Cracking and ultimate loads of test specimens

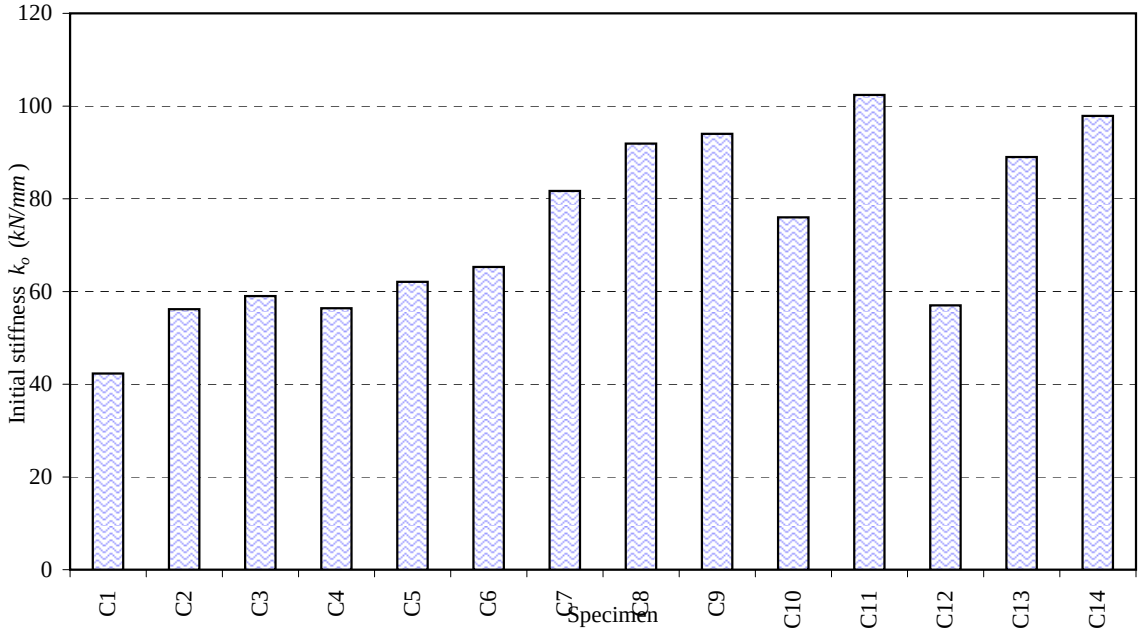

Fig. 5-3 Initial stiffness of test specimens

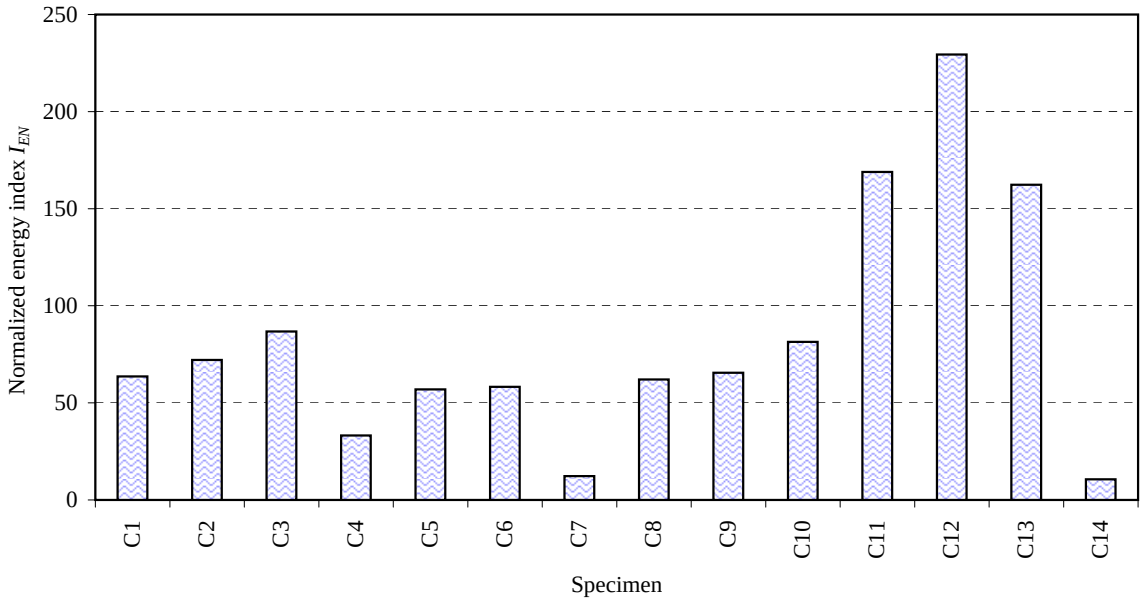

Fig. 5-4 Normalized energy index of test specimens

C14

C14

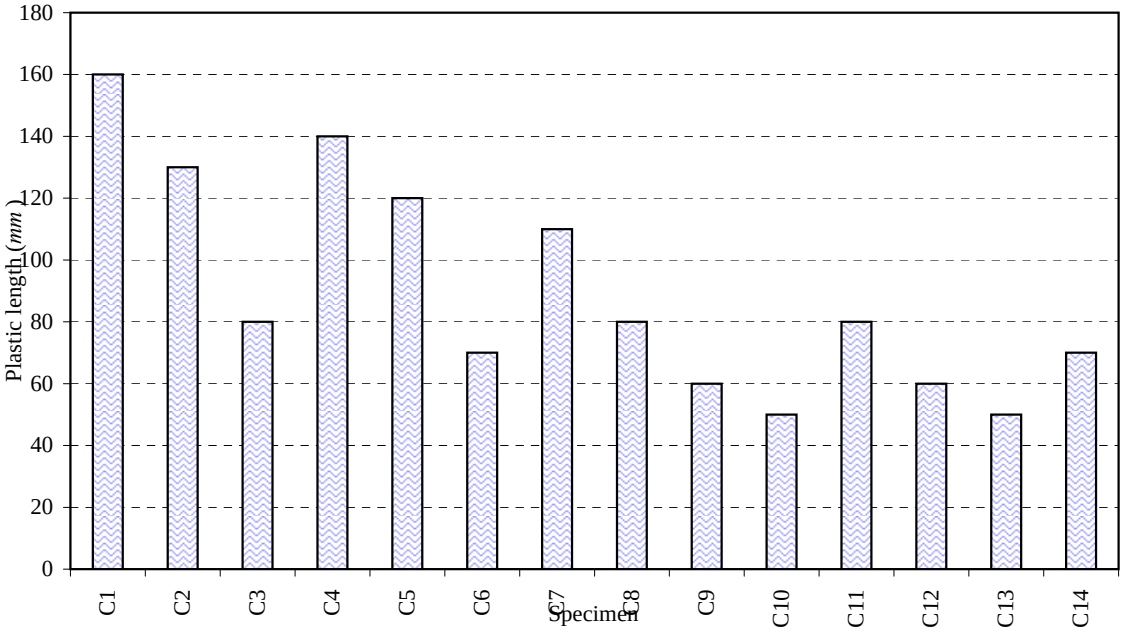

Fig. 5-5 Plastic length of test specimens

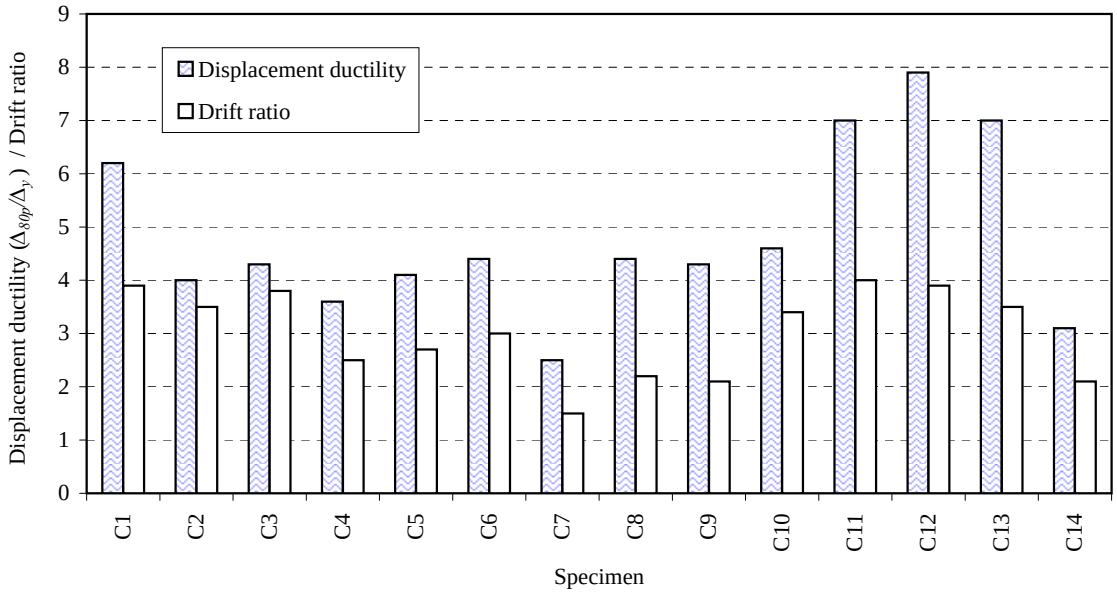

Fig. 5-6 Displacement ductility and Drift ratio of test specimens

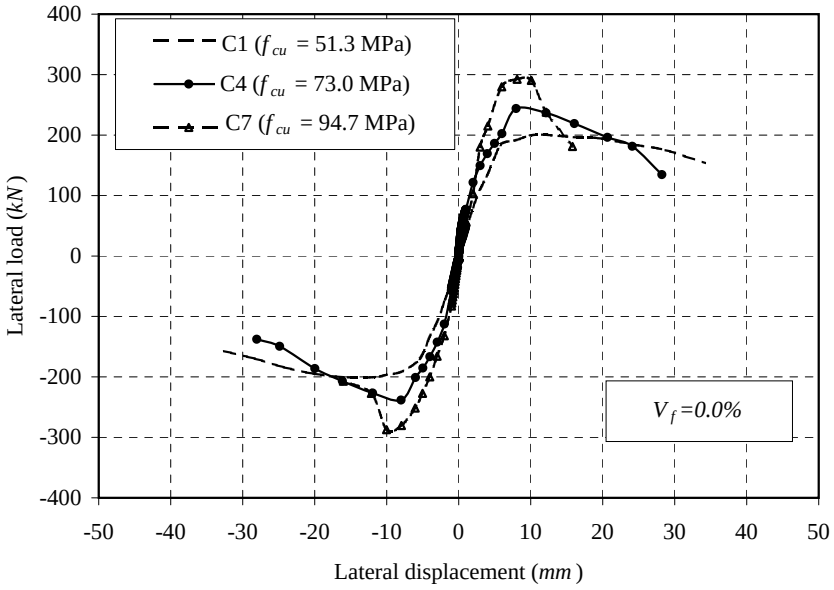

a)

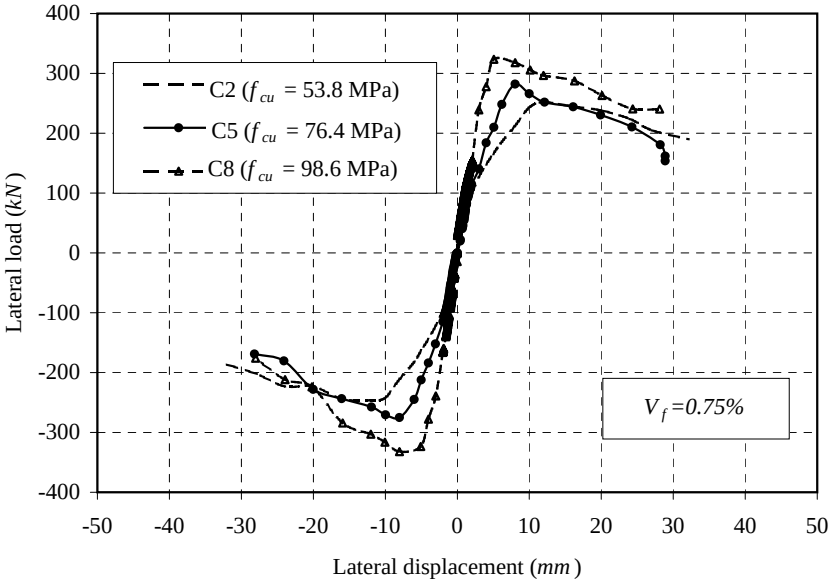

b)

Fig. 5-7 Effect of concrete compressive strength on load-displacement response of specimens with steel fibers content: a) 0.00%; b) 0.75%; c) 1.50%

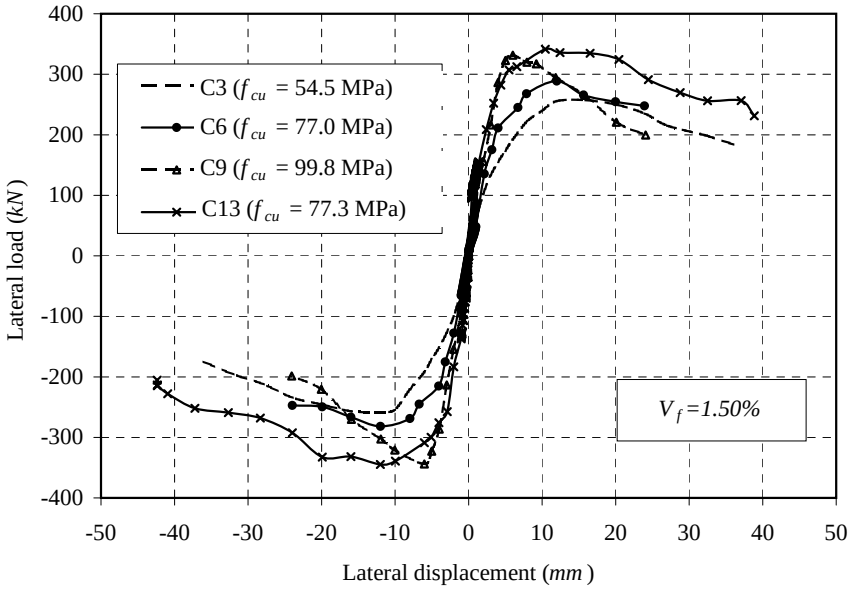

c)

Fig. 5-7 Effect of concrete compressive strength on load-displacement response of specimens with steel fibers content: a) 0.00%; b) 0.75%; c) 1.50% (cont.)

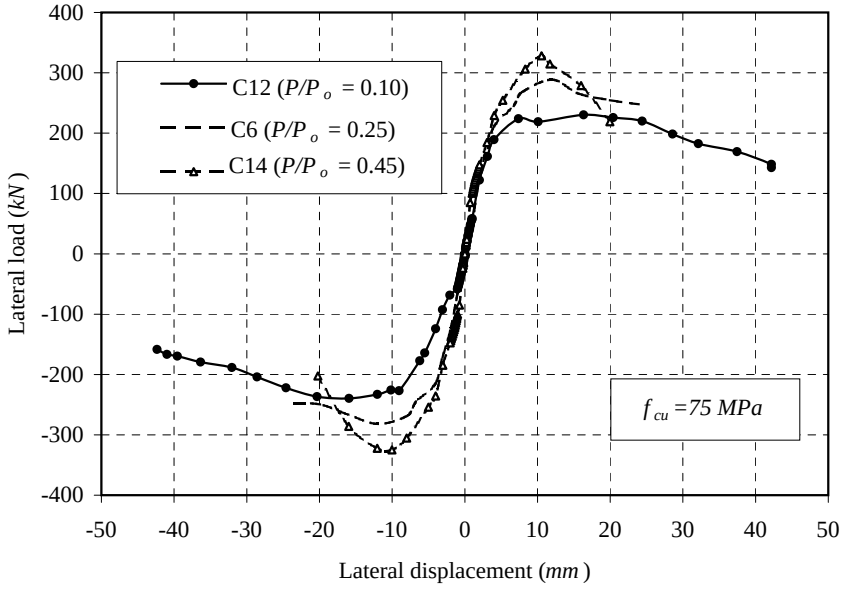

a)

Fig. 5-8 Effect of axial load level on load-displacement response of specimens with nominal concrete strength: a) 75 MPa; b) 100 MPa

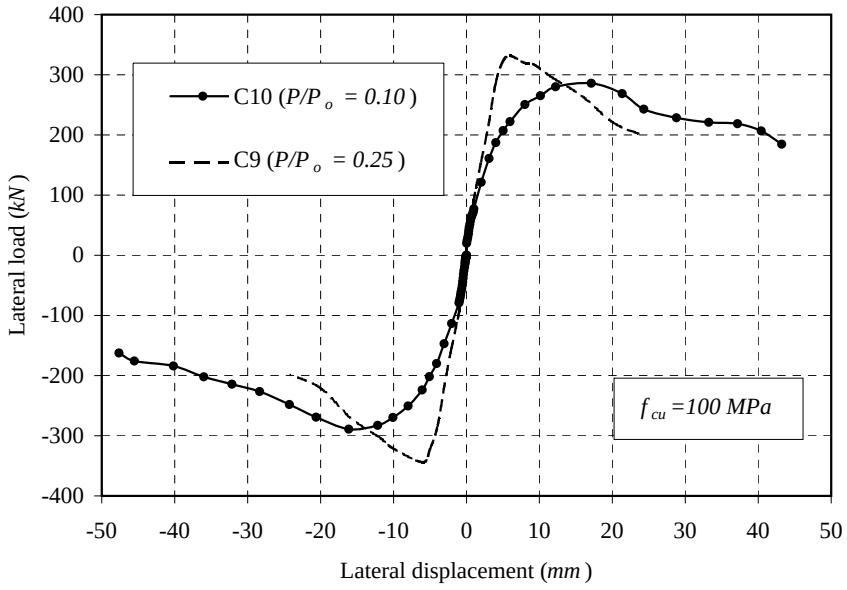

b)

Fig. 5-8 Effect of axial load level on load-displacement response of specimens with nominal concrete strength: a) 75 MPa; b) 100 MPa (cont.)

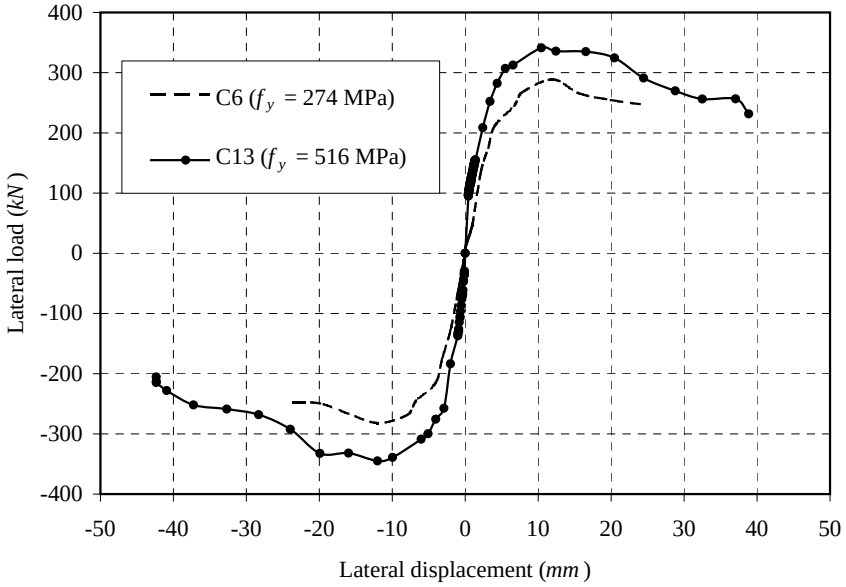

Fig. 5-9 Effect of yield strength of transverse reinforcement on load-displacement response

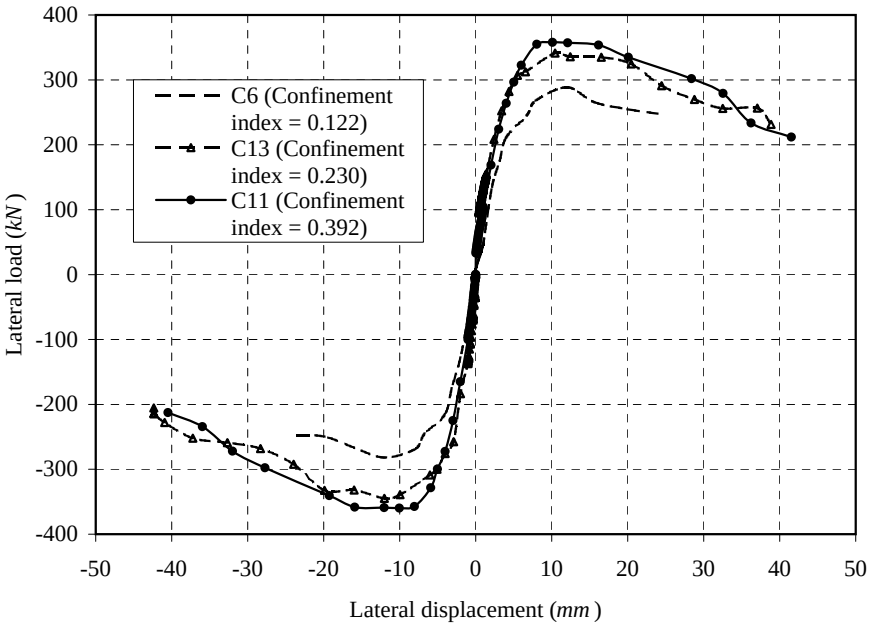

Fig. 5-10 Effect of confinement index on load-displacement response